PROCEEDINGS OF SCIENCE

Sterile neutrinos along the DUNE decay pipe

João Penedo[a] **and João Pulido**[a,b,*]

[a] *Centro de Física Teórica de Partículas, Instituto Superior Técnico, Av. Rovisco Pais, 1049-001, Lisboa, Portugal*

[b] *Centro de Física Teórica de Partículas, Instituto Superior Técnico, Av. Rovisco Pais, 1049-001, Lisboa, Portugal*

E-mail: joao.t.n.penedo@tecnico.ulisboa.pt, pulido@cftp.ist.utl.pt

We analyse the sensitivity of the Deep Underground Neutrino Experiment (DUNE) to a sterile neutrino, combining information from both the Near Detector (ND) and the Far Detector (FD). DUNE's sterile exclusion reach is affected by taking into account the information on the neutrino production point, in contrast to assuming a point-like neutrino source. Visible differences remain after taking into account energy bin-to-bin uncorrelated systematics.

8th Symposium on Prospects in the Physics of Discrete Symmetries (DISCRETE 2022)
7-11 November, 2022
Baden-Baden, Germany

*Speaker

PoS(DISCRETE2022)080

The first hint for sterile neutrinos came from the LSND experiment in which an intense proton beam hitting a target ultimately produced ν_μ, $\bar{\nu}_\mu$, ν_e and e^+ from $\pi^+ \to \mu^+\nu_\mu$ and $\mu^+ \to e^+\nu_e\bar{\nu}_\mu$ decays [1]. The unexpected observation of $\bar{\nu}_e$'s ($\bar{\nu}_e$ appearance) yielded the hypothesis that some of the $\bar{\nu}_\mu$'s could oscillate into $\bar{\nu}_e$'s through sterile neutrinos. More recently, it has been noted that sterile neutrinos also provide a viable explanation for the Gallium and reactor antineutrino anomalies (for a review see [2]). For the first of these, artificial neutrino radioactive sources were placed inside the GALLEX [3] and SAGE [4] Ga detectors for calibration in order to measure the reaction $\nu_e + {}^{71}\mathrm{Ga} \to e^- + {}^{71}\mathrm{Ge}$. A deficit of the observed rate with respect to the well measured activity of the sources was found: $\bar{R} = 0.844 \pm 0.031$ for the dominant Ge ground state production mode, with the contributions to its excited states being very similar [5]. For the reactor antineutrino anomaly (RAA) [6], fewer than expected antineutrinos from radioactive nuclides in the reaction $\bar{\nu}_e + p \to e^+ + n$ were found, with $\bar{R} = 0.936 \pm^{0.024}_{0.023}$ [7]. A possible solution to this ν_e ($\bar{\nu}_e$) disappearance is to introduce one sterile neutrino (3+1 scenario) with

$$\Delta m^2_{41} \simeq \Delta m^2_{42} \simeq \Delta m^2_{43} = O(1\ \mathrm{eV}^2)\ ,\ \ \sin^2\theta_{14} \sim 0.1. \tag{1}$$

However, upon this assumption, a larger than 2σ tension arises between the Ga and RAA preferred values [5]

$$\Delta m^2_{41}(\mathrm{Ga}) \sim 2\Delta m^2_{41}(\mathrm{Reactor}) \quad \sin^2 2\theta_{14}(\mathrm{Ga}) \sim 3\sin^2 2\theta_{14}(\mathrm{Reactor}).$$

Given the order of magnitude of Δm^2_{41}, the possible active/sterile oscillations are short-baseline (SBL) and, if they exist, they must show up in ν_μ, $\bar{\nu}_\mu$ disappearance which has not been the case so far. On the other hand, in the approximation of small mixing, the following relation holds

$$\sin^2 2\theta_{e\mu} \simeq \frac{1}{4}\sin^2 2\theta_{ee}\sin^2 2\theta_{\mu\mu}$$

(with $\sin^2 2\theta_{e\mu} = \sin^2 2\theta_{14}\sin^2\theta_{24}$, $\theta_{ee} = \theta_{14}$, $\theta_{\mu\mu} \simeq \theta_{24}$). However, evidence from several experiments shows that [1]

- $\sin^2 2\theta_{e\mu} \gtrsim 10^{-3}$ from ν_e, $\bar{\nu}_e$ appearance (e. g. LSND, Karmen [8])
- $\sin^2 2\theta_{ee} \sim (0.15 - 0.2)$ from ν_e, $\bar{\nu}_e$ disappearance, however in tension (Ga, RAA)
- $\sin^2 2\theta_{\mu\mu} \lesssim 10^{-2}$ from ν_μ, $\bar{\nu}_\mu$ disappearance (e. g. MINOS&MINOS+ [9]).

Moreover, recent constraints on $\sin^2 2\theta_{e\mu}$ slightly contradict LSND [10]

$$\sin^2 2\theta_{e\mu} < 10^{-3}$$

unless $\Delta m^2_{41} > 3\ \mathrm{eV}^2$, which in turn implies a tension with Ga and reactor antineutrino anomalies. Hence the sterile neutrino issue remains unsettled.

To this end, the Deep Underground Neutrino Experiment (DUNE) setup [11], whose nominal mission is to perform precise measurements of neutrino properties and oscillations, may play an important clarifying role. In this experiment, neutrinos are produced from meson decays along a

[1] This list of experiments is by all means incomplete.

decay pipe originating from proton collisions on a graphite target (see fig.1), so the neutrino source is smeared in space rather than point-like. In the 3+0 case (no steriles), owing to the smallness of Δm^2's, no oscillations can occur up to the near detector (ND). On the other hand, in the 3+1 case active/sterile oscillations can take place upstream from the ND, since the order of magnitude of Δm^2_{41} $(0.1 - 1\ \mathrm{eV}^2)$ implies this oscillation length to be of the order of the decay pipe length.

Given the fact that the neutrino origin is distributed along the decay pipe (fig.2) and oscillation to steriles occurs prior to the ND, a point-source approximation would be erroneous and source-volume effects need to be explicitly taken into account. The objective of our present work is thus to evaluate the effect of sterile neutrinos in DUNE ND and FD event rates from a statistical analysis, assuming a neutrino smeared source.

Figure 1: Diagram of the DUNE beam setup, where z represents the distance from the graphite target.

We used the GLoBES software [13, 14] and conceptually divided the decay pipe into 30 sections, associating each to a different point-source with its fixed baseline L. The flux arriving at the ND from each section is passed to GLoBES as the flux of an independent experiment [2].

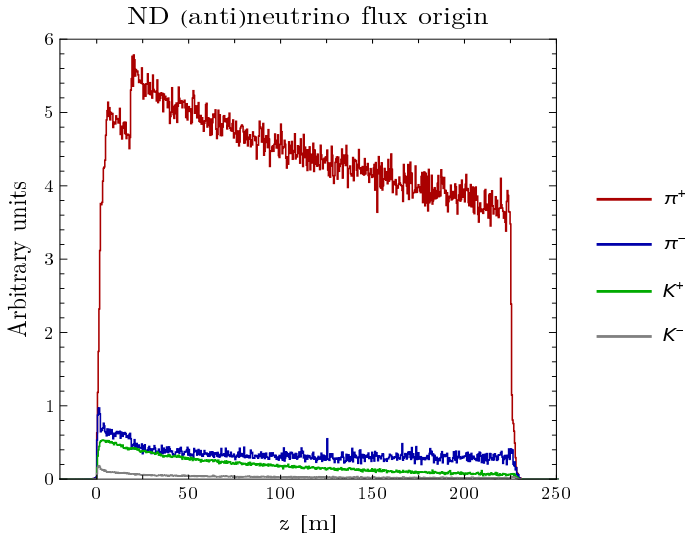

Figure 2: The origin of the neutrinos and antineutrinos from π and K decays reaching the ND.

In the 3+1 framework, the propagation of neutrinos in matter is described by the Hamiltonian $(\alpha, \beta = e, \mu, \tau, s)$

$$H^{\mathrm{mat}}_{\alpha\beta} = \frac{1}{2E}\left[U\ \mathrm{diag}(0, \Delta m^2_{21}, \Delta m^2_{31}, \Delta m^2_{41})U^{\dagger} + \mathrm{diag}(A_{CC}, 0, 0, A_{NC})\right] \tag{2}$$

[2] GLoBES internal functions are modified so that one effectively works with two experiments/detectors when computing χ^2.

where U is the Pontecorvo-Maki-Nakagawa-Sakata (PMNS) matrix, $A_{CC} = 2\sqrt{2}G_F N_e E$, $A_{NC} = \sqrt{2}G_F N_n E$ and N_e, N_n are the electron and neutron densities in the medium ($N_e \simeq N_n$). The matter Hamiltonian (2) can be brought, apart from a constant term which does not affect the oscillation probabilities, to a vacuum form (identical to the first term in (2)) with the replacements $U \to \tilde{U}$, $\Delta m^2_{ij} \to \Delta \tilde{m}^2_{ij}$ where the tildes denote the values of these quantities in matter. Denoting the eigenvalues of the matrix $2EH^{\text{mat}}$ by $\hat{\Delta} m^2_{i1}$ ($i = 1, ..., 4$), eq.(2) becomes (for the analytical formulation see [15]),

$$H^{\text{mat}}_{\alpha\beta} = \frac{1}{2E}\left[U\ \text{diag}(0, \Delta\tilde{m}^2_{21}, \Delta\tilde{m}^2_{31}, \Delta\tilde{m}^2_{41})U^\dagger + \hat{\Delta} m^2_{11}\text{diag}(1,1,1,1)\right]. \tag{3}$$

At the ND, the oscillation probability (short-baseline) depends on the point of production of the (active) α flavour neutrino, located at a distance $L = L_1 + L_2$. We have [15]

$$P^{SBL}_{\alpha\beta}(L_i, E) = \left| \sum_\gamma \sum_{j,k} \tilde{U}_{\beta j}\tilde{U}^*_{\gamma j} U_{\gamma k} U^*_{\alpha k} \exp\left(-i\frac{\Delta m^2_{k1}L_1 + \Delta\tilde{m}^2_{j1}L_2}{2E}\right)\right|^2 \tag{4}$$

where L_1 and L_2 denote the distances travelled by the neutrinos in vacuum and in matter up to the ND.

For both ND and FD event rates, a low-pass filter must be applied at the probability level to appropriately average out unresolvable fast oscillations. At the FD, the rates are expected to be sensitive simply to the matter density, $\rho \simeq 2.6$ g cm^{-3}, so only the $\tilde{U}$'s and the $\Delta\tilde{m}^2$'s remain in the long baseline (LBL) probability expression

$$P^{LBL}_{\alpha\beta}(L, E) = \sum_{j,j'} \tilde{U}_{\beta j}\tilde{U}^*_{\alpha j}\tilde{U}_{\alpha j'}\tilde{U}^*_{\beta j'} \exp\left(-i\frac{\Delta\tilde{m}^2_{jj'}L}{2E}\right) \exp\left[-\frac{\sigma^2_E}{2E^2}\left(\frac{\Delta\tilde{m}^2_{jj'}L}{2E}\right)^2\right] \tag{5}$$

for a single baseline L in matter. Here the rightmost exponential is a Gaussian low-pass filter averaging out the fast oscillations [16].

For the ND event rate, matter effects are negligible and it is enough to consider the following approximate result obtained in the limit of vanishing matter density and vanishing standard neutrino mass squared differences [15].

$$P^{SBL}_{\alpha\beta}(L, E) \simeq \delta_{\alpha\beta} - 2|U_{\alpha 4}|^2\left(\delta_{\alpha\beta} - |U_{\beta 4}|^2\right)\left\{1 - \cos\left(\frac{\Delta m^2_{41}L}{2E}\right)\exp\left[-\frac{\sigma^2_E}{2E^2}\left(\frac{\Delta m^2_{41}L}{2E}\right)^2\right]\right\}. \tag{6}$$

In the 3+0 case at the ND and in forward horn current (FHC) mode, where the dominant process is $\pi^+ \to \mu^+\nu_\mu$, the signal event rate is composed solely of ν_μ, whereas in reverse horn current (RHC) mode, with $\pi^- \to \mu^-\bar{\nu}_\mu$ as the dominant process, it is solely $\bar{\nu}_\mu$. In the 3+0 case at the FD and in FHC the signal is ν_μ and ν_e (due to oscillations) and correspondingly in RHC it is $\bar{\nu}_\mu$ and $\bar{\nu}_e$.

However, background from contamination ($\nu_e, \bar{\nu}_e$) and misisdentifications ($\nu_\mu, \bar{\nu}_\mu$ misidentified as $\nu_e, \bar{\nu}_e$) are present in both detectors and operation odes (FHC and RHC), and are therefore part of the event rates.

We consider the 3+1 case and follow the DUNE simulation configurations. For the statistical analysis, the concept of 'channel' and 'rule' are essential. A 'channel' consists of the physical

oscillation process, the energy reconstruction and the detection process (neutral or charged current)[3], whereas a 'rule' consists of a number of signal and background channels and their associated systematical uncertainties. Rules constitute the final link between the event rate and the statistical analysis. Hence, schematically

Rule (event rate ∪ stat. analysis): signal, bkg, syst. uncertainties

For each of the two operation modes (FHC and RHC), two rules are to be considered: for FHC the search is driven to neutrinos, while for RHC it is driven to antineutrinos. Hence there will be four rules altogether

- FHC whose signal is ν_e (at the ND this signal is only possible in the 3+1 case)
- RHC whose signal is $\bar{\nu}_e$ (at the ND this signal is only possible in the 3+1 case)
- FHC whose signal is ν_μ
- RHC whose signal is $\bar{\nu}_\mu$

All other channels in each of these rules are considered background. Note however that rules are not 100% efficient: some $\bar{\nu}$'s and ν's contaminate FHC and RHC respectively.

We use the following definition of χ^2

$$\chi^2 = \chi^2_{\text{stat}}(\omega, \omega_0, \zeta, \zeta') + \chi^2_{\text{prior}}(\omega, \omega_0) + \sum_{k=1}^{26}\left(\frac{\zeta_k}{\sigma_k}\right)^2 + \sum_{r=1}^{4}\sum_{i=1}^{60}\left(\frac{\zeta'_{r,i}}{\sigma'}\right)^2 \tag{7}$$

for 60 energy bins (i) with energy $E_i \in [1.25, 18.0]$ GeV in each rule (r). Two different possibilities were investigated: one in which energy bin errors are neglected and one with bin-to-bin uncorrelated shape uncertainties $\zeta'_{r,i}$ with $\sigma' = 5\%$. In eq.(7), ω denotes the 7 measured random parameters $\Delta m^2_{21}, \Delta m^2_{32}, \theta_{12}, \theta_{13}, \theta_{23}, \rho_{ND}, \rho_{FD}$ with central values ω_0; ζ_k are the 26 normalization random parameters (ND and FD fiducial volumes, fluxes, cross sections) with their respective standard deviations σ_k given in table 3 of ref. [12][4]. The statistical analysis proceeds with either $(\Delta m^2_{41}, \theta_{14})$ or $(\Delta m^2_{41}, \theta_{24})$ fixed, marginalizing respectively over θ_{24} or θ_{14} totally unconstrained along with all other parameters, namely $\theta_{34}, \delta_{14}, \delta_{24}$, also unconstrained. We have therefore 7+26+1+3+240=277 marginalized random parameters. The χ^2 minimization appears to be insensitive to the value of δ_{CP}, which we fix at 1.28π. The statistical and prior χ^2 contributions in eq.(7) are given by

$$\chi^2_{\text{stat}} = 2\sum_{d=1}^{2}\sum_{r=1}^{4}\sum_{i=1}^{60}\left[T^d_{r,i} - O^d_{r,i}\left(1 - \ln\frac{O^d_{r,i}}{T^d_{r,i}}\right)\right] \quad , \quad \chi^2_{\text{prior}} = \sum_{j=1}^{7}\left(\frac{\omega_j - (\omega_0)_j}{\sigma(\omega_j)}\right)^2 \tag{8}$$

with the test and observed event rates for each detector d

$$T^d_{r,i} = \sum_{\text{c=s,b}} N^d_{r,c,i}(\omega)\left(1 + \zeta'_{r,c,i} + \sum_{(k)}\zeta\right) \quad , \quad O^d_{r,i} = \sum_{\text{c=s,b}} N^d_{r,c,i}(\omega_0) \tag{9}$$

where the subscript $c = s, b$ denotes signal and background and $\sum_{(k)}\zeta$ is restricted to those ζ_k parameters involved in d, c, r.

[3] In our analysis we restrict ourselves to charged current (CC) processes.

[4] See also table 1 of [15].

Searching for $\chi^2_{min} = 4.61$ (2 d.o.f.), we get the sterile neutrino exclusion plots (figs.3,4).

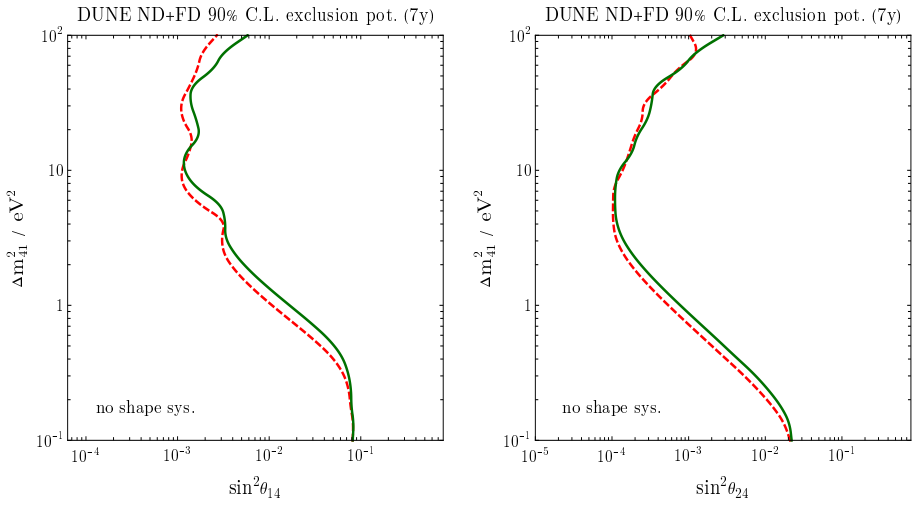

Figure 3: The sterile exclusion potential of the combined DUNE ND and FD CC analyses at 90% CL after 7 years of operation with no ζ' systematics. The dashed red curves are obtained assuming a common baseline $L = 574$ m for ND oscillations and the solid green curves consider the smeared-source effect.

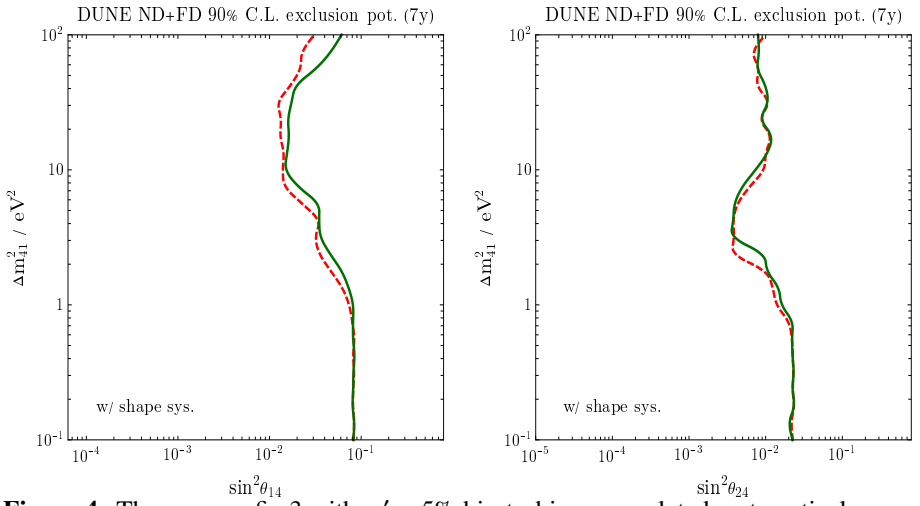

Figure 4: The same as fig.3 with $\sigma' = 5\%$ bin-to-bin uncorrelated systematical errors.

Summarizing our main conclusions

- We considered the effect of a spatial distribution in the oscillation baseline for sterile neutrinos instead of a single baseline.
- We took into account both DUNE ND and FD event rates with and without energy shape systematics.
- Consequently, DUNE's sterile neutrino exclusion reach is affected with a slight decrease in sensitivity, relevant for precision studies.
- This effect is present both with and without energy shape systematics.

Acknowledgments

We thank the organizers of Discrete 2022 for providing us with the opportunity to present our results. We are also indebted to Sampsa Vihonen for extensive support and insighful discussions. J.T.P. further thanks M. Orcinha for assistance with ROOT. The work of J.T.P. was supported by Fundação para a Ciência e Tecnologia (FCT, Portugal) through the projects PTDC/FIS-PAR/29436/2017, CERN/FIS-PAR/0004/2019 and CFTP Unit 777 (namely UIDB/00777/2020 and UIDP/00777/2020 which are partially funded through POCTI (FEDER), COMPETE, QREN and EU. CFTP computing facilities were extensively used throughout the project.

References

[1] C. Athanassopoulos *et al.* [LSND], "Evidence for anti-muon-neutrino —> anti-electron-neutrino oscillations from the LSND experiment at LAMPF," Phys. Rev. Lett. **77** (1996), 3082-3085 [arXiv:nucl-ex/9605003 [nucl-ex]].

[2] C. Giunti and T. Lasserre, "eV-scale Sterile Neutrinos," Ann. Rev. Nucl. Part. Sci. **69** (2019), 163-190 [arXiv:1901.08330 [hep-ph]].

[3] F. Kaether, W. Hampel, G. Heusser, J. Kiko and T. Kirsten, "Reanalysis of the GALLEX solar neutrino flux and source experiments," Phys. Lett. B **685** (2010), 47-54 [arXiv:1001.2731 [hep-ex]].

[4] J. N. Abdurashitov *et al.* "Measurement of the response of a Ga solar neutrino experiment to neutrinos from an Ar-37 source," Phys. Rev. C **73** (2006), 045805 [arXiv:nucl-ex/0512041 [nucl-ex]].

[5] C. Giunti, Y. F. Li, C. A. Ternes, O. Tyagi and Z. Xin, "Gallium Anomaly: critical view from the global picture of ν_e and $\overline{\nu}_e$ disappearance," JHEP **10** (2022), 164 [arXiv:2209.00916 [hep-ph]].

[6] G. Mention, M. Fechner, T. Lasserre, T. A. Mueller, D. Lhuillier, M. Cribier and A. Letourneau, "The Reactor Antineutrino Anomaly," Phys. Rev. D **83** (2011), 073006 [arXiv:1101.2755 [hep-ex]].

[7] C. Giunti, Y. F. Li, C. A. Ternes and Z. Xin, "Reactor antineutrino anomaly in light of recent flux model refinements," Phys. Lett. B **829** (2022), 137054 [arXiv:2110.06820 [hep-ph]].

[8] B. Armbruster *et al.* [KARMEN], "Upper limits for neutrino oscillations muon-anti-neutrino —> electron-anti-neutrino from muon decay at rest," Phys. Rev. D **65** (2002), 112001 [arXiv:hep-ex/0203021 [hep-ex]].

[9] P. Adamson *et al.* [MINOS+], "Search for sterile neutrinos in MINOS and MINOS+ using a two-detector fit," Phys. Rev. Lett. **122** (2019) no.9, 091803 [arXiv:1710.06488 [hep-ex]].

[10] P. Adamson *et al.* [MINOS+ and Daya Bay], "Improved Constraints on Sterile Neutrino Mixing from Disappearance Searches in the MINOS, MINOS+, Daya Bay, and Bugey-3 Experiments," Phys. Rev. Lett. **125** (2020) no.7, 071801 [arXiv:2002.00301 [hep-ex]].

[11] B. Abi *et al.* [DUNE], "Experiment Simulation Configurations Approximating DUNE TDR," [arXiv:2103.04797 [hep-ex]].

[12] B. Abi *et al.* [DUNE], "Prospects for beyond the Standard Model physics searches at the Deep Underground Neutrino Experiment," Eur. Phys. J. C **81** (2021) no.4, 322 [arXiv:2008.12769 [hep-ex]].

[13] P. Huber, M. Lindner and W. Winter, "Simulation of long-baseline neutrino oscillation experiments with GLoBES (General Long Baseline Experiment Simulator)," Comput. Phys. Commun. **167** (2005), 195 [arXiv:hep-ph/0407333 [hep-ph]].

[14] P. Huber, J. Kopp, M. Lindner, M. Rolinec and W. Winter, "New features in the simulation of neutrino oscillation experiments with GLoBES 3.0: General Long Baseline Experiment Simulator," Comput. Phys. Commun. **177** (2007), 432-438 [arXiv:hep-ph/0701187 [hep-ph]].

[15] J. T. Penedo and J. Pulido, "Baseline and other effects for a sterile neutrino at DUNE," [arXiv:2207.02331 [hep-ph]].

[16] GLoBES manual, version `3.2.18`, `www.mpi-hd.mpg.de/personalhomes/globes/documentation/globes-manual-3.2.18.pdf`